



ELSEVIER

Contents lists available at ScienceDirect

Materials Science & Engineering C

journal homepage: <http://ees.elsevier.com>

Bioinspired avian feather designs

Tarah N. Sullivan, Tzu-Tying Hung, Audrey Velasco-Hogan, Marc A. Meyers*

University of California, San Diego, La Jolla, CA, USA

ARTICLE INFO

Keywords

Bioinspired design
Avian feather
Adhesive
Nanocomposite

ABSTRACT

Avian flight feathers have developed, through evolution, an intricate architecture with multi-functional structures that are essential for flight. These lightweight and resilient appendages motivate the invention of bioinspired designs. Here we fabricate various structures inspired by significant concepts identified in the feather vane and shaft. Bioinspired prototypes based on the feather vane's unique adhesive mechanism and directional permeability are explored, and feather-shaft inspired designs motivated by the highly ordered hierarchical fiber-matrix structure in the feather are fabricated. The exquisite architecture of the rachis, consisting of a hollow tube filled with foam, is simulated in a bioinspired design that demonstrates the synergy of the two components in enhancing the flexural strength. These structures provide an enhanced understanding of the mechanisms operating in feathers and suggest highly efficient solutions which can contribute to creating innovative materials inspired by the feather.

1. Introduction

Evolved for lightweight strength, the avian flight feather's elegant design serves as a springboard for innovation. These β -keratinous structures are considered essential to bird flight, comprising the majority of the wing and allowing for lift [1]. The flight feather consists of a main shaft (rachis and calamus) and a vane composed of barbs that branch from the rachis and barbules that branch from barbs (Fig. 1) [2,3]. Microhooks and grooves at the ends of barbules hold barbs cohesively together forming a tight-knit vane for the effective capture of air. This highly hierarchical design of the modern feather arose during the Late Jurassic period with the progression of avian aerial locomotion [4]. Prior to the C-T extinction, pterosaurs had developed the ability to fly, but their unique wings were composed of a long framework covered with a specialized skin and muscle tissue [1]. The evolutionary success of the feather for flight can be gauged by the large number of bird species: over 10,000 [5].

Recent developments revealing the structural and material properties of the feather are leading to the creation of bioinspired designs. These designs distill a few relevant aspects of the feather from its highly complex structure, and can lead to novel synthetic architectures and a deeper understanding of the feather itself. Here, we discuss our recent advances in bioinspired feather designs based on progression in the understanding of some of the most important structural features of the feather.

2. Materials and methods

2.1. Bioinspired feather vane fabrication

Bioinspired feather vanes were drawn in the Computer Aided Design program SolidWorks (SolidWorks Corp., MA, USA) and fabricated via 3D-printing. All the models were designed on an enlarged scale in order to be able to observe the mechanics of the structures. The initial interlocking barbule bioinspired structure was printed with ABS plastics, with an elastic modulus ~ 2 GPa, using an ABS-M30 printer (Stratasys, MN, USA). Flexible barbule hooks and grooves were printed using thermoplastic polyurethane NinjaFlex filament, with an elastic modulus ~ 12 MPa, (NinjaTek, PA, USA) with a Makerbot 3D printer (MakerBot Industries, NY, USA). The remaining barbule inspired designs were 3D-printed using a Stratasys Objet260 Connex3 printer (Stratasys, MN, USA), TangoBlack and VeroClear (Stratasys, MN, USA) filament as well as combinations of the two were used to print the structures, with the elastic modulus ranging from 0.2 MPa to 2 GPa. It is important to note that the elastic modulus of keratin, the constituent material of feathers, is ~ 2.5 GPa. While there is a mismatch in materials properties of the printed material and keratin, the crux of this work is to extract the defining design motifs, not to replicate direct copies.

* Corresponding author.

Email address: mameyers@eng.ucsd.edu (M.A. Meyers)

[Edit](#)[Proof](#)[PDF](#)

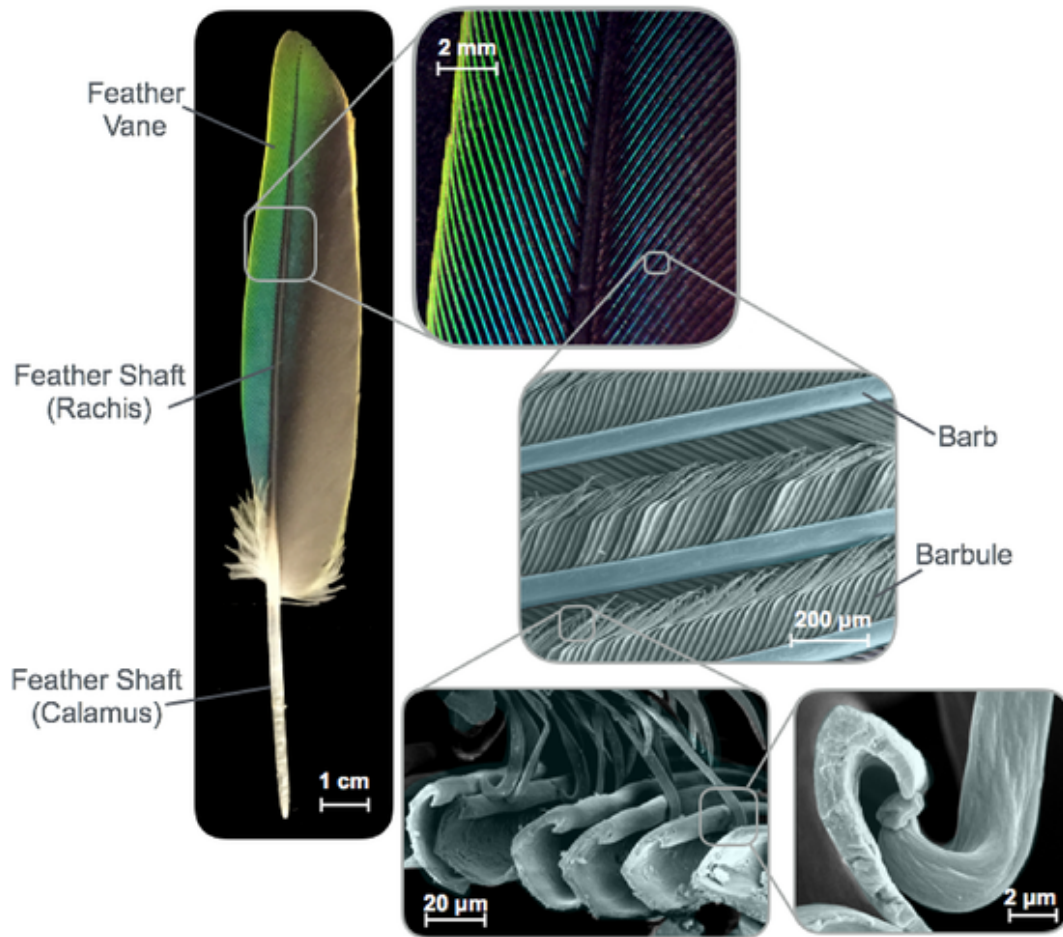


Fig. 1. The hierarchical structure of the flight feather. This efficient structure consists of the main shaft (rachis and calamus) and the vane. Within the vane, barbs branch from the rachis and barbules stem from barbs. Barbules are hooked on one side and grooved on the other providing an interlocking material that effectively captures air. Image taken from [20].

2.2. Bioinspired feather shaft fabrication

Bioinspired composite feather shafts were fabricated by coating polyethylene foam cylinders (Foam Factory, MI, USA) with layers of unidirectional S-glass fiberglass (ACP Composites, CA, USA) and epoxy resin system 2000 with hardener 2020-A (Fibre Glast, OH, USA). Bioinspired rachis were designed in SolidWorks (SolidWorks Corp., MA, USA) and printed using a Stratasys Objet260 Connex3 printer with RGD8730 filament, with an elastic modulus of ~ 0.2 MPa (Stratasys, MN, USA). After printing, support material was removed using a water jet followed by soaking in 4% NaOH solution for 72h. The Samples were dried overnight before mechanical testing.

2.3. Characterization of the feather vane and shaft

Sections of the feather were sliced with a razor blade, mounted to a stub and imaged using scanning electron microscopy (SEM). The dimensions of sections were measured using the software ImageJ (National Institutes of Health, MD, USA).

2.4. Three-point bending of the bioinspired rachis

Three-point bending tests were performed using a mechanical testing machine, Instron 3367 load frame (Instron, High Wycombe, United Kingdom), with a 30 kN load cell. Three samples of each prototype

were tested (with foam and without foam) with a support span (L) of 128mm. A load was applied with a constant speed of 4.26mm/min. The force-displacement curves and failure mechanisms were highly repeatable and consistent for all samples.

3. Results and discussion

3.1. Hook-and-groove barbule inspired designs

Interlocking hook-and-groove structures within the feather vane inspired the creation of several bioinspired designs, which progressively exhibit improved performance. By examining SEM images, microscopic barbules are observed to have multiple hooks branching from a single distal barbule to fit securely into grooved proximal barbules (Fig. 2a). Both sets of barbules branch from barbs at an angle and slide along one another prior to detachment. It is important to note that the following designs are simplifications of the feather architecture and are not intended to be duplications. We extract what we believe to be the defining design motifs and scale it up in size to better understand mechanisms involved. While the feather relies on bunches of hooklets to adhere we focus on a discrete hooklet and groove pattern for ease in manufacturing. From these initial observations, the first bioinspired model of the barbule structure was fabricated through 3D printing and is $20 \times 20 \times 3.5$ cm when interlocked (Fig. 2b) [6]. While this bioinspired structure illustrates the general mechanism by which the feather vane maintains cohesiveness, it does not incorporate the elastic response of unzipping the feather into its design because it is composed of rigid ABS plastics.

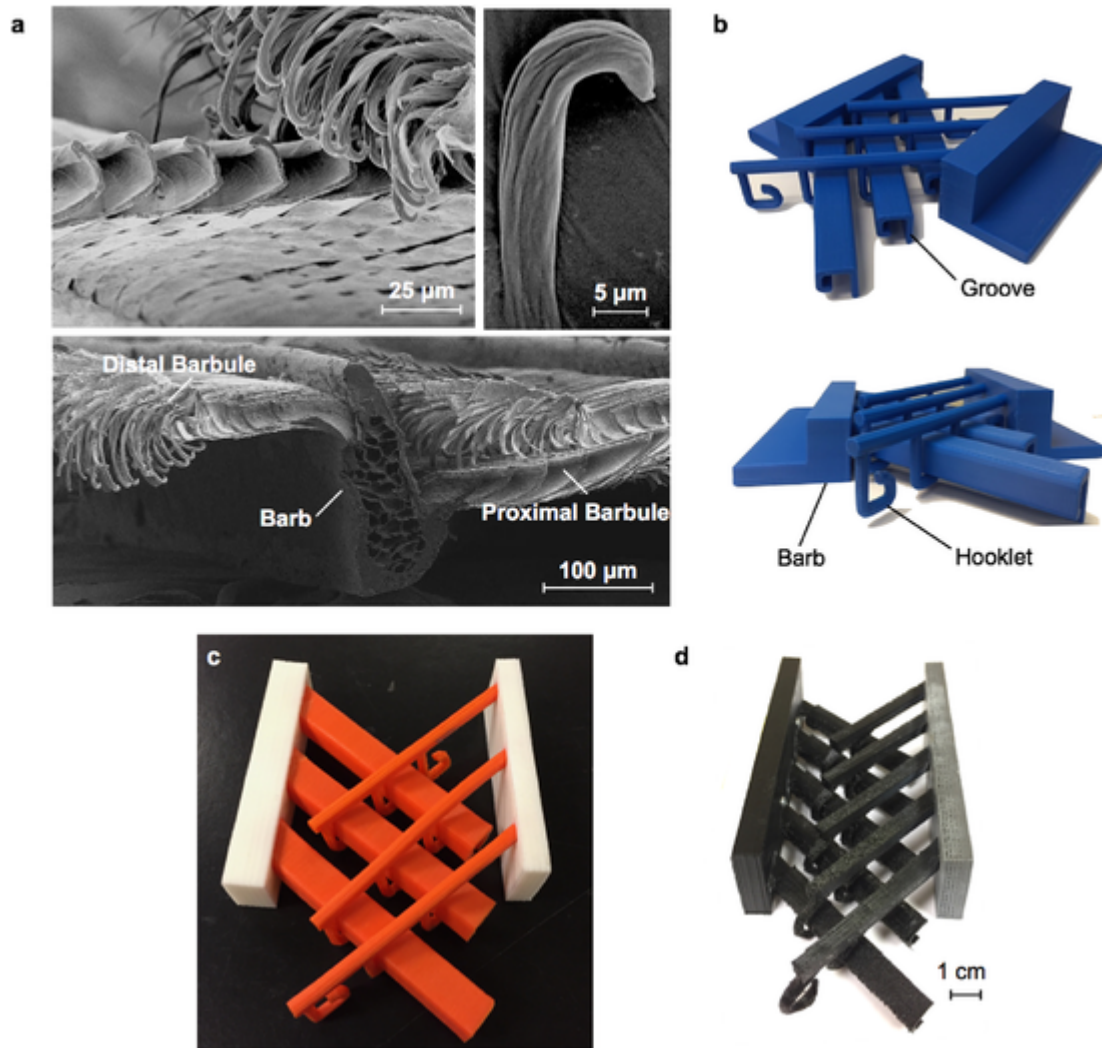


Fig. 2. Interlocking barbules and bioinspired designs. (a) Micrographs of the California seagull (*Larus californicus*) (top, left) and the American white pelican (*Pelecanus erythrorhynchos*) (top, right and bottom) show barbule hooks and grooves within the feather vane. (b) This interlocking mechanism was simplified and then reconstructed using additive manufacturing to create a three-dimensional model. (c) The original hook and groove design was printed with flexible material. (d) A design with thinner hooks and grooves allowed for increased flexibility in the model. Panel b is taken from [6].

In an attempt to mimic the stiffness (or compliance) of barbule connections, hook and grooved barbules were printed with a flexible material (NinjaFlex) (when interlocked this model is 8.5×13×2.5 cm) (Fig. 2c). In this model, however, the thick groove structure is too rigid to flex when barbules were unzipped, and therefore does not exhibit the elastic response witnessed in the feather vane. Following this, hooks and grooves were altered to have a thinner, more flexible structure and were 3D printed using the flexible filament material (NinjaFlex), yielding a vane with an elastic response when separated (Fig. 2d). This model is 9×17×3.5 cm when interlocked. Several hook designs were printed and mechanically tested in adhesion to find that hooks with increased curvature allow for enhanced attachment to grooves [7].

3.2. Barbule-inspired designs with membrane flaps

Research on the directional permeability of the feather vane revealed the importance of the membrane flaps that extend from each barbule [7]. These flaps act as one-way valves, allowing air to flow dorsally through the vane but not ventrally (Fig. 3a,b). Thus, air is efficiently captured when the bird is executing a down stroke, but is allowed to pass through in the upstroke. A bioinspired model of barbules

with these flaps was 3D printed using flexible material (Stratasys FLX9095) and measures at 23×17×2 cm (Fig. 3c,d). This model demonstrates directional permeability, as shown in Fig. 3d. Dorsal airflow forces flaps to bend backward and allow air through, yet with ventral airflow the flaps remain closed, capturing air. Finally, a complete feather structure was 3D printed (measuring 12×23×1.5 cm at its largest dimensions) (Fig. 3e) with barbules composed of stiff material to permit hooks and grooves to slide along one another; barbules made of flexible material allow for bending so that barbules can detach, and membrane flaps printed with a flexible material allow for opening with dorsal airflow. This structure offers a simplified yet effective visual description of the complex nature of the feather vane.

3.3. Barbule-inspired designs to allow for tailored air permeability

Analysis of 3D printed models reveals that the feather vane may have two levels of control over air permeability. First, as previously discussed, membrane flaps of barbules allow for air to flow through the space between barbules dorsally but not ventrally. Second, as hooks slide along grooves, expansion within the feather vane offers another level of tailored permeability; when hooks are slid close to the base of

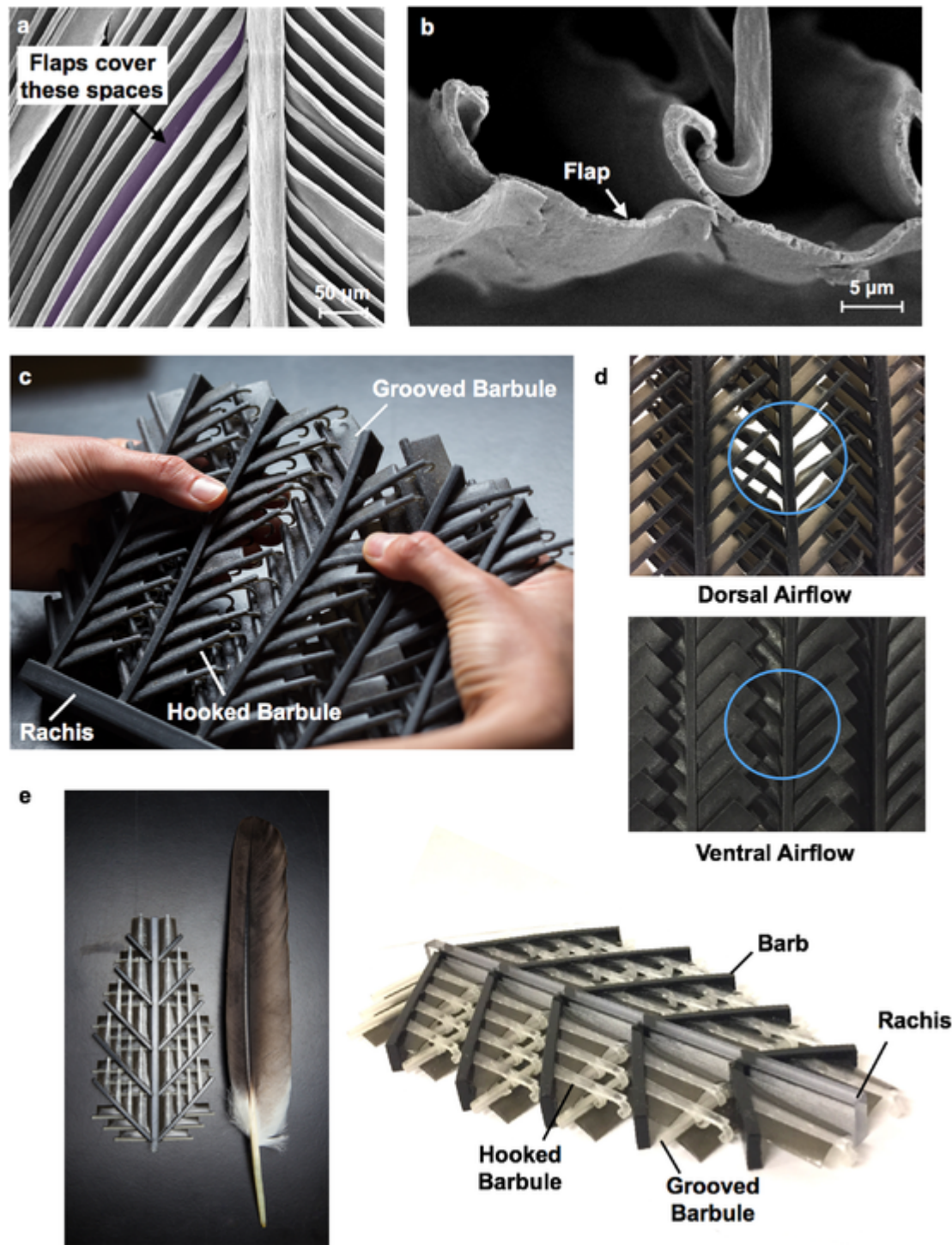


Fig. 3. Membrane flaps in the feather vane for increased efficiency. The directional permeability in the feather vane is due to membrane flaps that extend from barbules to act as one-way valves covering the space between barbules. Scanning electron micrographs show these flaps in the vane of the Crested guinea fowl (*Guttera pucherani*) and the House sparrow (*Passer domesticus*) (a,b respectively). (c) A simplified 3D printed model of the feather vane, and (d) the reaction of membrane flaps as air is blown dorsally (top) and ventrally (bottom) where blue circles represent air flow. (e) An entire feather was 3D printed using a variety of materials. Image d is from [7]. (For interpretation of the references to colour in this figure legend, the reader is referred to the web version of this article.)

the groove, the vane is much tighter than when they are at the tip of the groove, nearly ready to detach. This behavior was used to create a bioinspired design. Fig. 4a shows an assembly of barbules attached on either end with a flexible material. As this is stretched, they slide along one another leading to controlled openings between each barb's set of

barbules. Fig. 4b shows the opening within the vane by stretching, indicated by the four hands pulling it apart. This model is $25 \times 20 \times 3$ cm.

Hooks are identified as a weak point of this design, because their slender dimensions lead them to break easily. To overcome this, another, exclusively groove-based, structure was created where each groove slides into a groove on the neighboring barb (Fig. 4c,d) (this

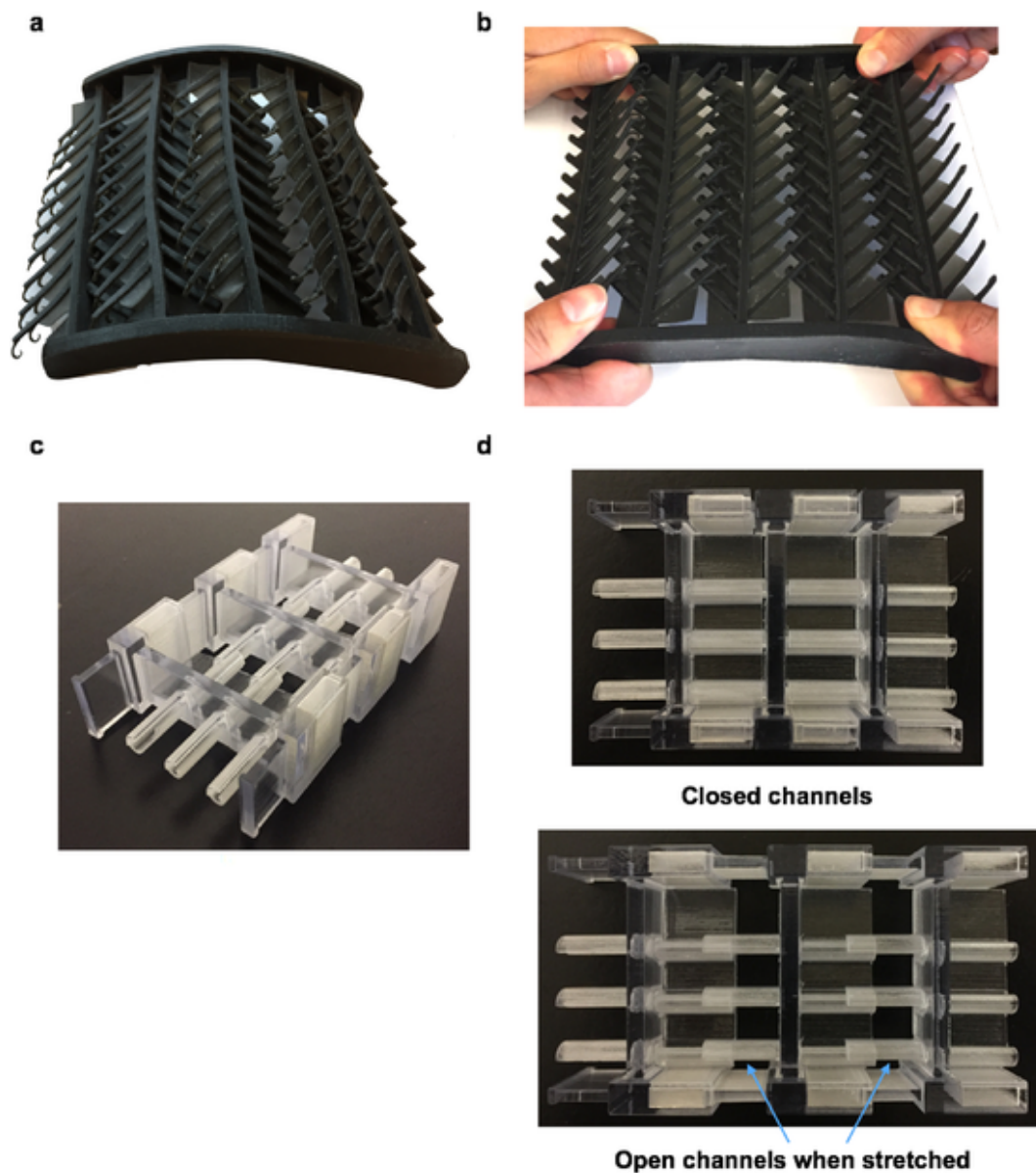


Fig. 4. Membrane flaps are incorporated into the 3D printing design to create directional permeability. (a) Barbules are bounded on both ends with a flexible material, (b) when these ends are pulled apart, feather become more permeable as space between each barb's barbules opens. (c,d) Grooved structures that slide along one another were created to allow for a design that has tailored permeability based on the distance edges are pulled apart from one another.

model is $9.5 \times 5 \times 2$ cm when pulled apart). These structures are not able to completely detach due to stoppers placed at the end of each groove. Adding this feature makes the design more amenable to real-world applications where tailored permeability is desired, but complete material detachment is detrimental.

To aid in ease of manufacturing, yet display the same behavior, a square tubing model ($11 \times 6 \times 1.5$ cm when fully stretched apart) was created that allows for increased permeability when pulled apart (Fig. 5a). Squares slide within hollow tubes until they are stopped at the end of the tubing, behaving similarly to a piston. This model is scaled down further ($16.5 \times 8.5 \times 0.7$ cm) (Fig. 5b), to create a design that expands to $\sim 20\%$ of its original length and is able to have a maximum curvature that is double (Fig. 5c) when completely outstretched (with open channels) than when compressed. The design's flexibility in the direction of sliding is demonstrated in Fig. 5d. One of the shortcomings of this design is that it maintains a rigid structure in the direction perpendicular to sliding. To allow for flexibility in both directions, the design

was altered to have sliding square tubes in two dimensions (Fig. 6). This two-dimensional sliding structure elongates $\sim 27\%$ from its original length in each dimension, behaving as a textile when stretched open (Fig. 6d) due to the increase in spacing between rigid sections. This model is $11.5 \times 11.5 \times 0.4$ cm when fully stretched.

A tridimensional structure was printed by using elements similar to the chainmail-like design, but incorporating sliding in a third dimension so that it can be manipulated in all three dimensions. This cube is displayed in Fig. 7 with its bottom right corner compressed and top left corner stretched in Fig. 7b. When compressed, this model is a $7.5 \times 7.5 \times 7.5$ cm cube. While this design may not be readily recognizable as the hook and groove derivative from the feather, it is associated with a similar underlying function. This is essential to bioinspired design which prospers from creativity and distancing from direct replication. It is important to remind ourselves of the interconnectedness of nature and that similar design motifs can be found across a diverse range of biological materials. For example, this structure is reminiscent

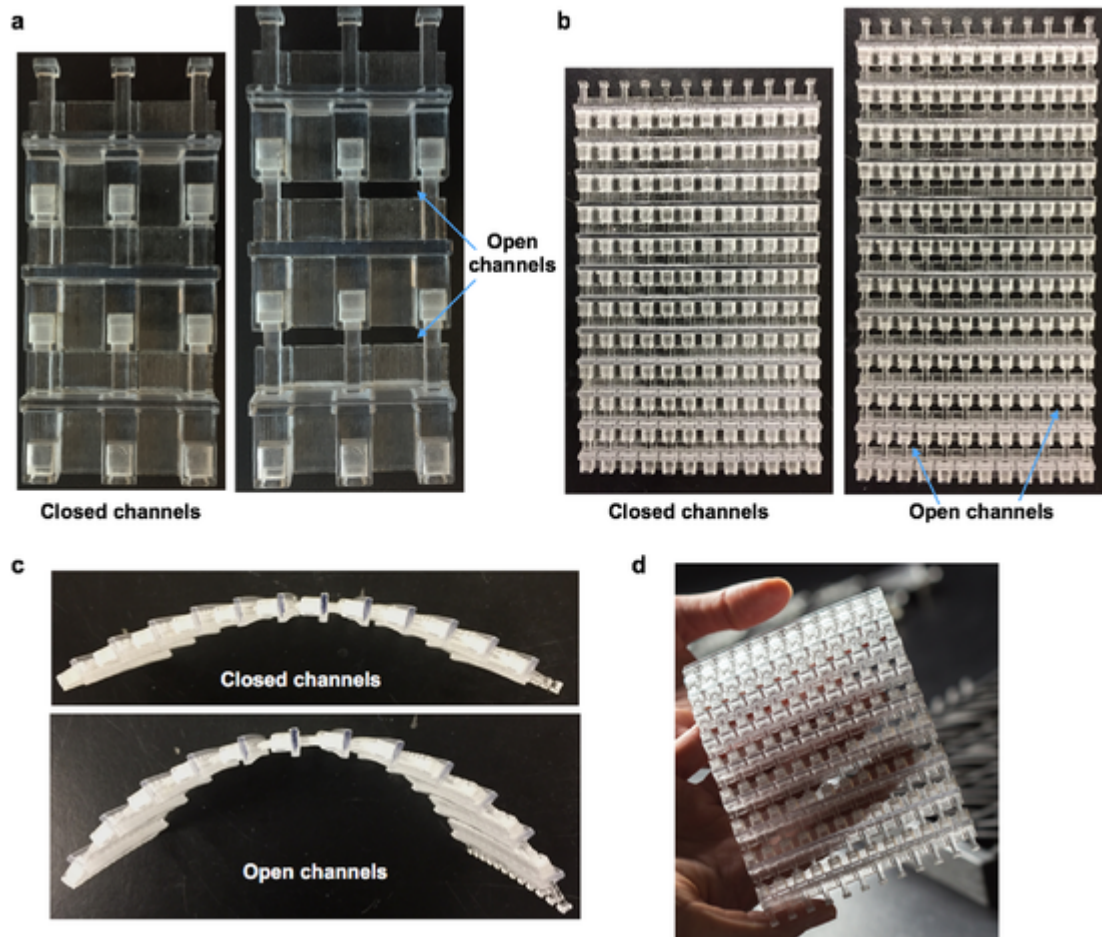


Fig. 5. The square tubing bioinspired model. (a) Squares slide through tubes and are stopped at the end, which allows the material to have tailored permeability depending on the degree to which the material is stretched. As the structure is scaled down further (b) it is able to develop a curvature with open channels twice that of with closed channels (c). The flexibility of the design is demonstrated (d).

to the smart material inspired by the pine cone's permeability to humidity [8]. However, our structure differs from the pine cone inspired smart material, which is actuated by hydration, while here the stimulation is mechanical. The complex nature of barbules provides fertile ground for insight into new designs for a wide variety of applications. The feather shaft also serves as a source of inspiration due to its nanocomposite structure and is discussed in the next section.

3.4. Bioinspired feather shaft: calamus and rachis

The feather shaft is hierarchically organized; β -keratin filaments (~ 3 nm in diameter) form macrofibrils (~ 50 – 400 nm), which bundle to form fibers (~ 3 – 5 μ m) as shown in Fig. 8a [8–12]. The orientation of these fibers varies throughout the feather shaft. In the calamus fibers run longitudinally and circumferentially along the shaft, and in the rachis they alternate at angles of $\pm 45^\circ$ along the lateral walls (Fig. 8) [13,14]. The circumferential fibers prevent longitudinal fibers from splitting in flexure, while the angled fibers in the rachis provide torsional stiffness with minimal impact on the dorsal-ventral stiffness [15] and tailor the lateral flexural stiffness. It has been demonstrated that the organization of this biological composite varies slightly between bird species and is possibly related to the flight style of the bird [16,17]. Perhaps as a result of this variation, the Elastic modulus of β -keratin has been shown to differ between species of birds [18].

The organization of these fibers motivated the fabrication of foam-filled fiberglass-epoxy composites with shaft-inspired laminar designs.

As shown in Fig. 9, four feather-shaft inspired beams have fibers oriented in varying directions. The first beam contains only longitudinal fibers, the second has fibers running circumferentially around the shaft; in the third fibers run at 45° along the shaft, and the fourth beam is composed of longitudinal fibers surrounded by circumferential fibers. Each of these beams reflects the orientation of fibers in a section of the feather shaft or serves as a means of comparison. Composite structures with fiber directions analogous to those witnessed in the feather shaft are used commonly in the design of synthetic composites.

The architecture of the rachis is another source of inspiration. Disregarding the internal structure of organized filaments, bioinspired prototypes were fabricated with the intention of isolating the integral design motif which includes a reinforcing foam-filled center (Fig. 10). Two rachis-inspired designs were explored: (1) thin-walled-square-cross-section shells without foam-filled core and (2) with a foam-filled core (Fig. 10b). These architectures were mechanically tested using three-point bending to demonstrate that the presence of foam has an advantage by increasing the maximum force (F_{max}) and the maximum bending stress (σ_f) despite an increase in weight.

The stiffness (k) was calculated from the force-displacement curve in the elastic regime (Fig. 10a).

$$k = \frac{\delta F}{\delta x} \quad (1)$$

The stiffness of the foam-filled structures was not significantly different than the hollow shell with $p > 0.05$ (unpaired t -test, $p = 0.265$)

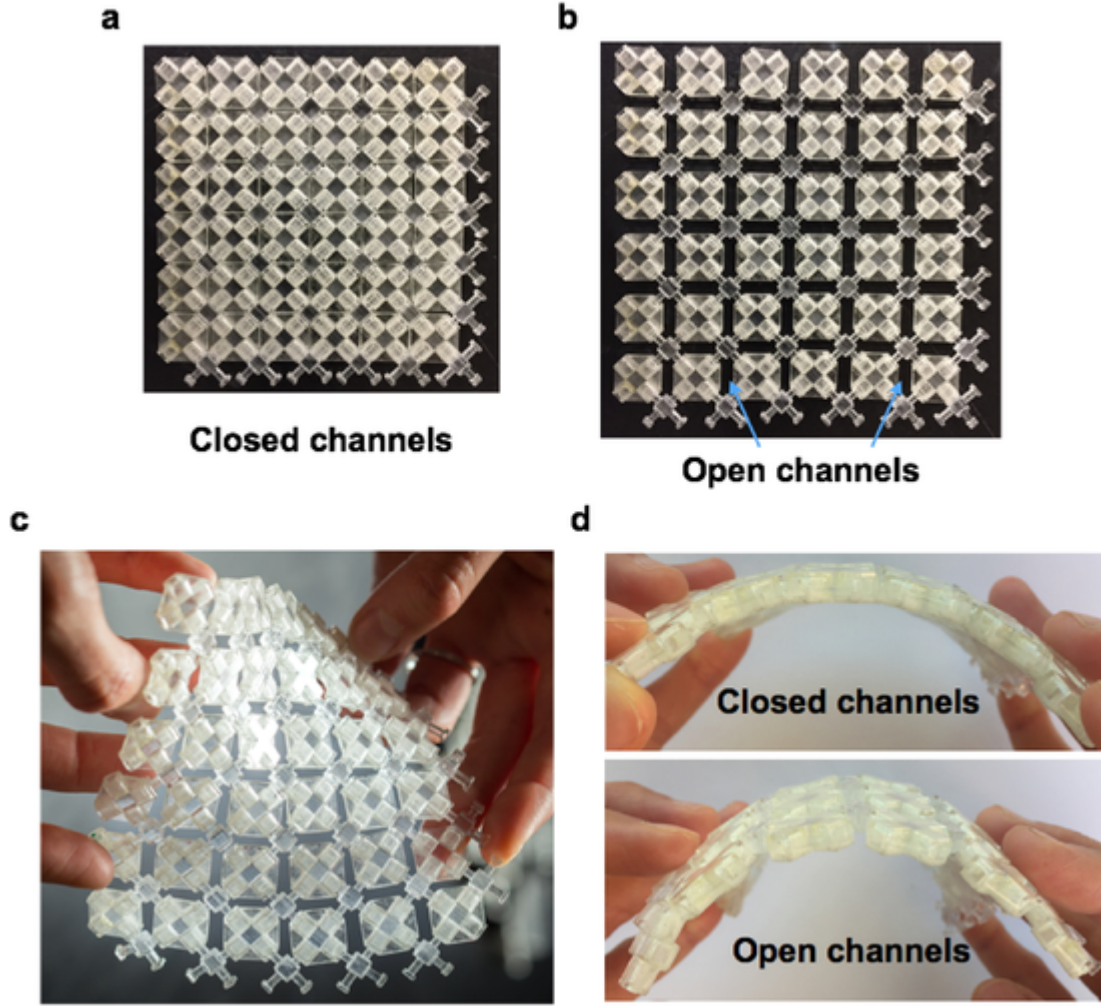


Fig. 6. Two-dimensional stretching for increased flexibility. (a,b) The square tubing model was altered to stretch in two directions, allowing for (c) a chainmail-like formable material composed of rigid pieces. (d) The maximum radius of curvature of the structure with closed and open channels.

(Fig. 10c). The foam does not contribute to the stiffness, since the stiffness of the shell is much greater than the stiffness of the foam.

While the foam does not influence the stiffness, it does affect the maximum force and the maximum bending stress. The foam-filled core acts as an elastic foundation that resists the buckling of the shell. The maximum bending stress of the hollow shell (σ_f^{hollow}) was calculated using the following:

$$\sigma_f^{hollow} = \frac{My}{I} \quad (2)$$

where M is the bending moment ($F_{max}L/4$), y is the vertical distance from the neutral axis, and I is the moment of inertia around the neutral axis. The maximum bending stress of the foam-filled structure was calculated using the following equations derived from Gibson and Ashby [19] for sandwich structure composites:

$$\sigma_f^{foam-filled} = \frac{My E_f}{(EI)_{eq}} \quad (3)$$

where,

$$EI_{eq} = \frac{E_f b t^3}{6} + \frac{E_c b c^3}{12} + \frac{E_f b t d^2}{2}, \quad (4)$$

and E_f and E_c are the Young's moduli of the face and the core, respec-

tively, b is the width, c is the thickness of the foam, d is the thickness of the sandwich composite, and t is the thickness of the shell (Fig. 10b).

The maximum force and maximum bending stress are significantly greater for the foam-filled shell than the hollow shell (Fig. 10d and e). Even when normalized for the additional weight of the foam, the maximum bending stress for the foam-filled composite is far superior to the hollow shell (Fig. 10f). This demonstrates that the addition of a foam core increases both the force and the maximum bending stress while maintaining a lightweight structure.

4. Conclusions: a path toward applications

Through evolution of over fifty million years, nature has developed unique structures and materials optimized for bird flight, resulting in great potential for the creation of novel, bioinspired designs based on the feather. Here, the feather vane is simplified to create barbule-inspired adhesive designs and structures with tailored permeability. These have possible applications in deployable structures, next-generation chainmail, and smart foams.

The structure created with two-dimensional sliding is reminiscent of chain-mail. This chainmail-like structure could serve as breathable armor, allowing for flexibility of conjoined rigid parts. Because the structure is able to change its size significantly by changing its shape, another possible application for the design is as a deployable structure for space-based applications. The three-dimensional structure could serve as a new "smart" foam design for shock absorbers that allows for com-

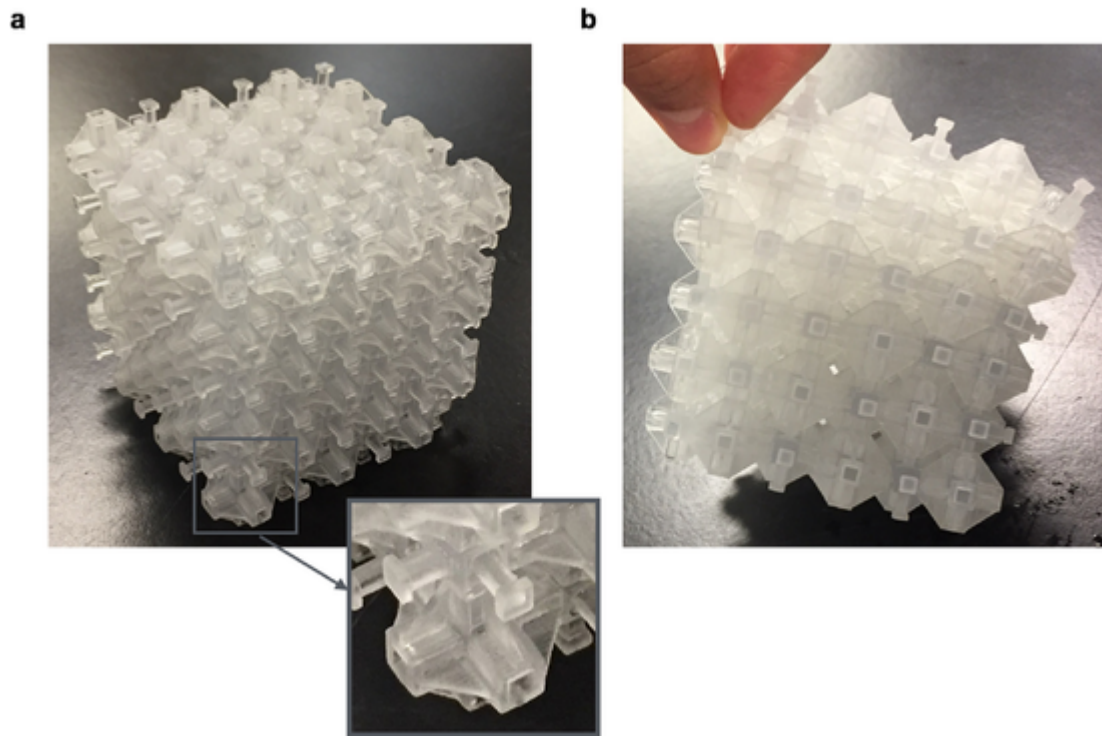


Fig. 7. Tridimensional bioinspired structure. (a) This cube is composed of elements that allow for sliding in three dimensions. (b) Compression of the right corner of the block is demonstrated, providing curvature to the shape.

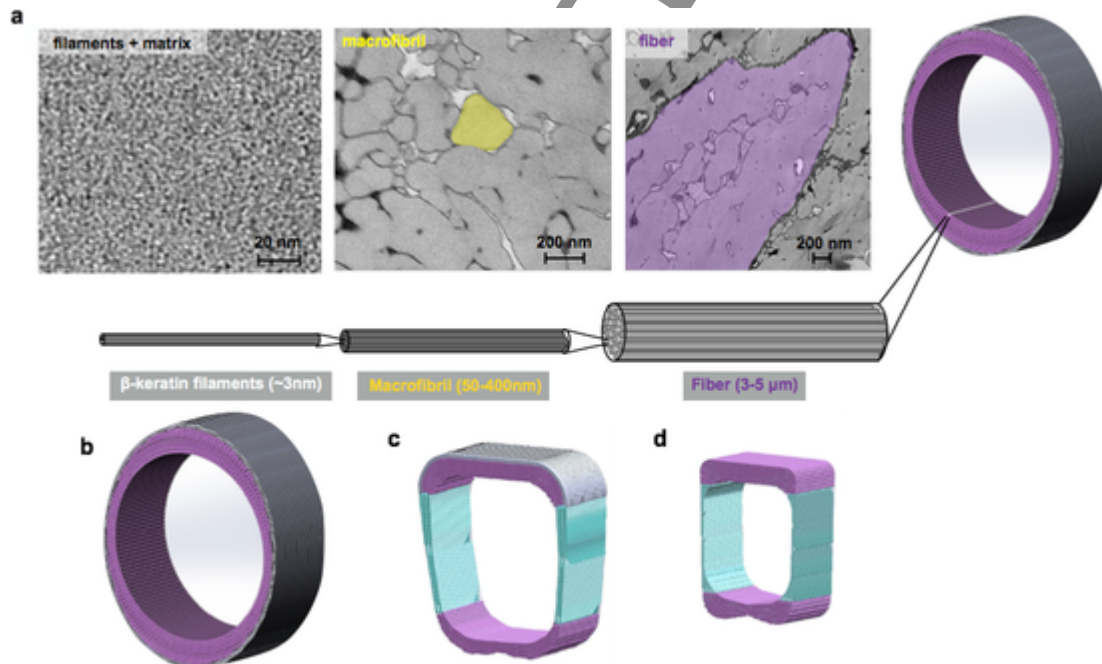


Fig. 8. The hierarchical structure of the feather shaft cortex. (a) β -keratin filaments form macrofibrils and these bundle to form fibers. The orientation of the fibers varies throughout the feather shaft: (b) fibers in the calamus (c) run longitudinally (purple) and circumferentially (grey), within middle and distal rachis (d) fibers alternate at angles $\pm 45^\circ$ (cyan) in the lateral walls. Image (a) from T.N. Sullivan et al. [21], (b–d) from B. Wang et al. [14]. (For interpretation of the references to colour in this figure legend, the reader is referred to the web version of this article.)

pression to occur only when sufficient force is applied to push each square through the hollow tube. Friction-inducing structures could be added to the ends of each square to tailor the force at which the structure will compress.

Bioinspired designs based on the feather have the potential to allow for the fabrication of new, lightweight materials for applications in industries ranging from aeronautical engineering to biomedical science. The feather is still rich in potential for novel bioinspired designs, and we anticipate that with advancements made in understanding the

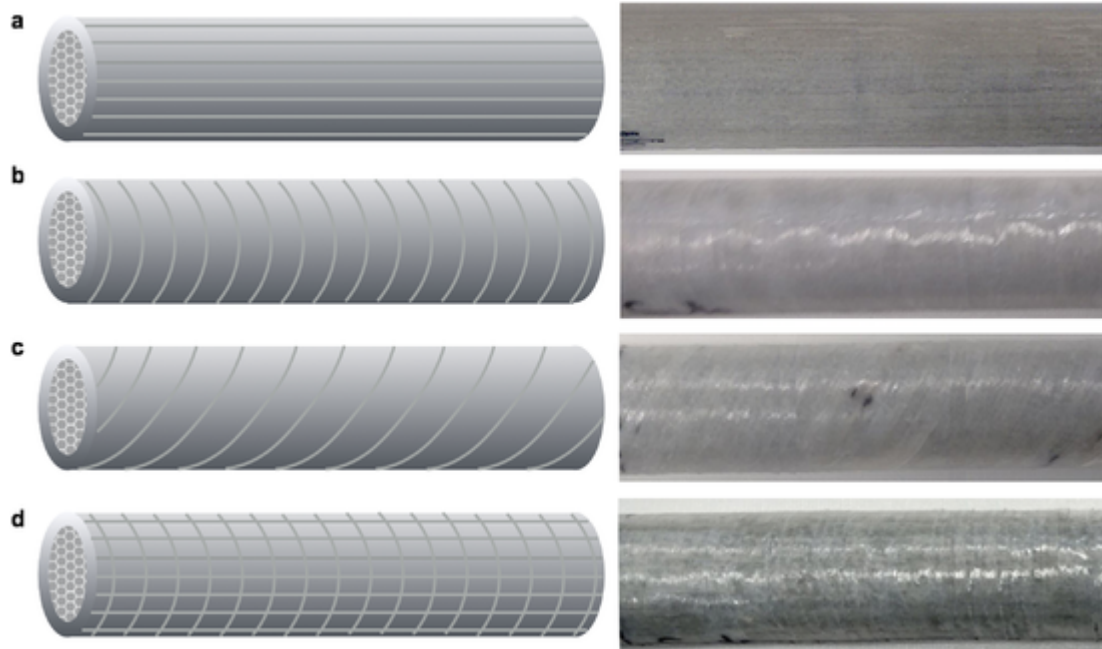


Fig. 9. Four cylindrical feather shaft-inspired designs. The design shown in (a) has fibers running longitudinally along the shaft, and (b) contains fibers running circumferentially around the shaft. In the structure shown in (c), fibers run at a 45° angle along the shaft, while (d) consists of two inner layers running along the axis of the shaft and a two outer layers running circumferentially around the foam.

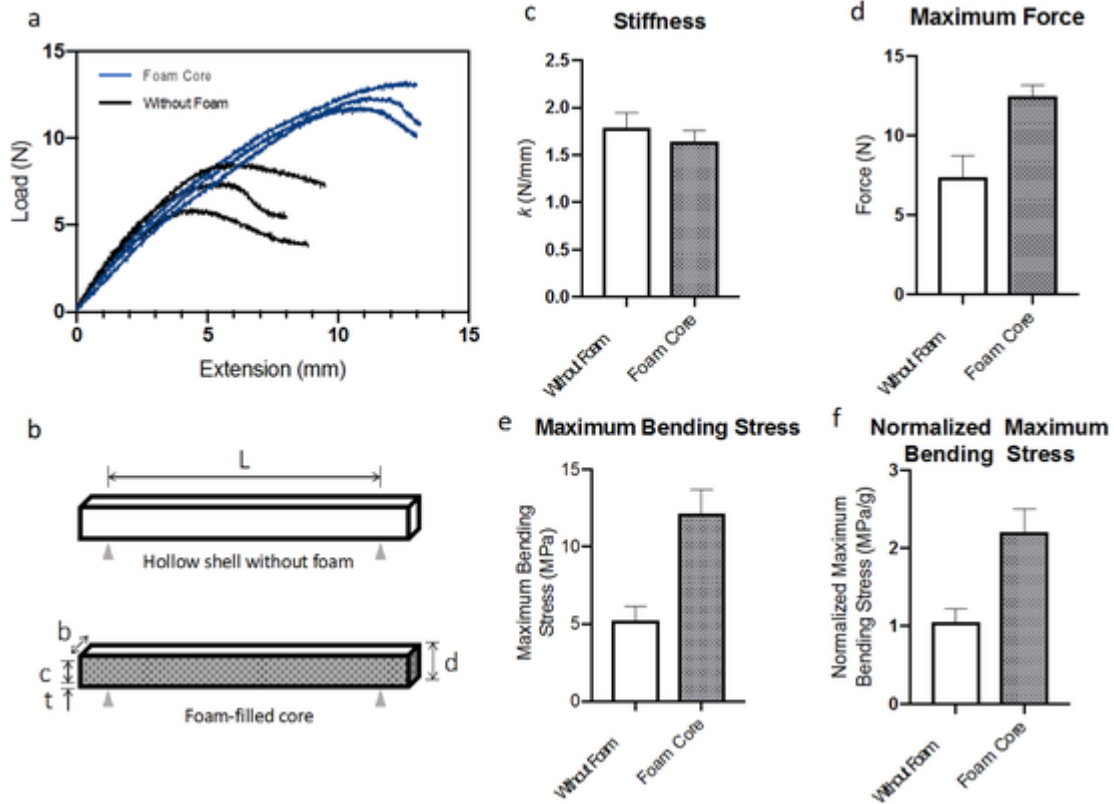


Fig. 10. Three-point bending of 3D-printed bioinspired rachis design. (a) Force-displacement curve from three-point bending of designs with foam (blue) and without foam (black) for three samples each. (b) Rachis bioinspired design with foam and without foam. (c) Stiffness values (mean \pm SD) for with foam and without foam. (d) Maximum force (mean \pm SD) for with foam and without foam. (e) Maximum bending stress (mean \pm SD) with foam and without foam. (f) Normalized Maximum bending stress (mean \pm SD) with foam and without foam. (For interpretation of the references to colour in this figure legend, the reader is referred to the web version of this article.)

feather, more innovative solutions will follow.

Acknowledgements

The authors thank generosity of Prof. Michael Tolley and his group for allowing us to use his equipment and Frances Su, Prof. Joanna McKittrick, Estelle Jouret, and Keenan Finney for discussions. We appreciate the help provided by Mauricio de Souza of Moura Boards in the fabrication of the feather-inspired cylinders. We thank the San Diego Zoo (April Gorow, Research Coordinator) and the San Diego Natural History Museum (Phil Unitt, Curator of Birds and Mammals) for providing feather samples to us. This work is supported by the AFOSR MURI (AFSOSR-FA9550-15-1-0009).

References

- [1] C.J. Pennycuik, *Modelling the Flying Bird*, 1st ed., Elsevier, Burlington, USA, 2008.
- [2] P.R. Stettenheim, The integumentary morphology of modern birds—an overview, *Am. Zool.* 40 (2000) 461–477.
- [3] F.B. Gill, *Ornithology*, second ed., W.H. Freeman, New York, USA, 1995.
- [4] J. Clarke, Feathers before flight, *Science* 340 (2013) 690–692.
- [5] J.J. Videler, Avian flight, in: T.R. Birkhead (Ed.), *Oxford Ornithol. Ser.*, Oxford University Press, Oxford, UK, 2005, pp. 2–7.
- [6] T.N. Sullivan, A. Pissarenko, S.A. Herrera, D. Kisailus, V.A. Lubarda, M.A. Meyers, A lightweight, biological structure with tailored stiffness: the feather vane, *Acta Biomater.* 41 (2016) 27–39.
- [7] T.N. Sullivan, M. Chon, R. Ramachandramoorthy, M.R. Roenbeck, T.-T. Hung, H.D. Espinosa, M.A. Meyers, Reversible attachment with tailored permeability: the feather vane and bioinspired designs, *Adv. Funct. Mater.* 27 (2017).
- [8] J.E. McMurry, R.C. Fay, *Chemistry*, 4th edition, Pearson Educ., 2004, doi:10.1017/CBO9781107415324.004.
- [9] R.D.B. Fraser, T.P. MacRae, G.E. Rogers, Keratins: Their Composition, Structure, and Biosynthesis, 52, 1972, pp. 29–30.
- [10] R.D.B. Fraser, D.A.D. Parry, The structural basis of the two-dimensional net pattern observed in the X-ray diffraction pattern of avian keratin, *J. Struct. Biol.* (2011), doi:10.1016/j.jsb.2011.08.010.
- [11] T. Lingham-Soliar, N. Murugan, A new helical crossed-fibre structure of β -keratin in flight feathers and its biomechanical implications, *PLoS One* (2013), doi:10.1371/journal.pone.0065849.
- [12] J. McKittrick, P.Y. Chen, S.G. Bodde, W. Yang, E.E. Novitskaya, M.A. Meyers, The structure, functions, and mechanical properties of keratin, *JOM* (2012), doi:10.1007/s11837-012-0302-8.
- [13] B. Wang, M.A. Meyers, Seagull feather shaft: correlation between structure and mechanical response, *Acta Biomater.* 48 (2016) 270–288.
- [14] B. Wang, M.A. Meyers, Light like a feather: a fibrous natural composite with a shape changing from round to square, *Adv. Sci.* 4 (2016).
- [15] T. Lingham-Soliar, Feather structure, biomechanics and biomimetics: the incredible lightness of being, *J. Ornithol.* 155 (2013) 323–336.
- [16] C.M. Laurent, C. Palmer, R.P. Boardman, G. Dyke, R.B. Cook, Nanomechanical properties of bird feather rachises: exploring naturally occurring fibre reinforced laminar composites, *J. R. Soc. Interface* 11 (2014).
- [17] B. Bussou, P. Engström, J. Doucet, Existence of various structural zones in keratinous tissues revealed by X-ray microdiffraction, *J. Synchrotron Radiat.* (1999), doi:10.1107/S0909049599004537.
- [18] P. Bonser, The Young's modulus of feather keratin, *J. Exp. Biol.* (1995).
- [19] L.J. Gibson, M.F. Ashby, *Cellular Solids: Structure and Properties*, second edition, 2014, doi:10.1017/CBO9781139878326.
- [20] T.N. Sullivan, B. Wang, H.D. Espinosa, M.A. Meyers, Extreme lightweight structures: avian feathers and bones, *Mater. Today* 20 (2017) 377–391.
- [21] T.N. Sullivan, Y. Zhang, P. Zavattieri, M.A. Meyers, Hydration-induced Shape and Strength Recovery of the Feather Submitted., 2018.